Published in final edited form as:

Nature. 2009 June 11; 459(7248): 871–874. doi:10.1038/nature07972.

An Unusual Carbon-Carbon Bond Cleavage Reaction During Phosphinothricin Biosynthesis

Robert M. Cicchillo[1,3,*], **Houjin Zhang**[2,5,*], **Joshua A.V. Blodgett**[4], **John T. Whitteck**[1,2], **Gongyong Li**[1], **Satish K. Nair**[2,3], **Wilfred A. van der Donk**[1,3], and **William W. Metcalf**[2,4]

[1]Department of Chemistry, University of Illinois at Urbana-Champaign, Urbana, IL 61801, USA

[2]Institute for Genomic Biology, University of Illinois at Urbana-Champaign, Urbana, IL 61802, USA

[3]Howard Hughes Medical Institute, University of Illinois at Urbana-Champaign, Urbana, IL 61802, USA

[4]Department of Microbiology, University of Illinois at Urbana-Champaign, Urbana, IL 61802, USA

[5]Department of Biochemistry, University of Illinois at Urbana-Champaign, Urbana, IL 61802, USA

Abstract

Natural products containing phosphorus-carbon bonds have found widespread use in medicine and agriculture1. One such compound, phosphinothricin tripeptide (PTT), contains the unusual amino acid phosphinothricin (PT) attached to two alanine residues (Fig. 1). Synthetic PT (glufosinate) is a component of two top-selling herbicides (Basta® and Liberty®), and is widely used with resistant transgenic crops including corn, cotton and canola. Recent genetic and biochemical studies showed that during PTT biosynthesis 2-hydroxyethylphosphonate (HEP) is converted to hydroxymethylphosphonate (HMP) (Fig. 1)2. Reported here are the *in vitro* reconstitution of this unprecedented C(sp^3)-C(sp^3) bond cleavage reaction and X-ray crystal structures of the enzyme. The protein is a mononuclear non-heme iron(II)-dependent dioxygenase that converts HEP to HMP and formate. In contrast to most other members of this family, the oxidative consumption of HEP does not require additional cofactors or the input of exogenous electrons. The current study expands the scope of reactions catalyzed by the 2-His-1-carboxylate mononuclear non-heme iron family of enzymes.

Correspondence and requests for materials should be addressed to S.K.N. (s-nair@life.uiuc.edu), W.A.V. (vddonk@illinois.edu) or W.W.M. (metcalf@illinois.edu).

*These authors contributed equally to this work.

Supplementary Information is linked to the online version of the paper at www.nature.com/nature.

Authors Contributions R.M.C. performed all biochemical assays shown, which were designed and analyzed by R.M.C and W.A.V. H.Z. and S.K.N. performed and interpreted all structural studies. W.W.M. designed and J.A.V. performed initial biochemical reactions and identified the products. J.T.W. and G.L. synthesized all substrates. R.M.C., S.K.N., and W.A.V. wrote the manuscript. R.M.C. and H.Z. contributed equally to this study.

Author Information Atomic coordinates and structure factors have been deposited in the Protein Data Base. Reprints and permissions information is available at www.nature.com/reprints

Hydroxyethylphosphonate dioxygenase (HEPD) was overexpressed in *E. coli* with an N-terminal hexa-histidine tag and purified by Ni^{2+}-affinity chromatography. As-isolated, the protein was inactive, but in the presence of Fe(II) and O_2 conversion of HEP to HMP was observed by ^{31}P NMR spectroscopy and high-performance liquid chromatography (HPLC). One molar equivalent of Fe(II) was sufficient for full reconstitution of activity. External reductants or cofactors were not required for catalysis, in contrast to most other non-heme iron(II) oxygenases3,4. Thus, all four electrons required for reduction of O_2 are provided by HEP.

The fate of the excised carbon was determined using synthetic 2-^{13}C-HEP. Stoichiometric amounts of HMP and a new product with a resonance of 171 ppm in the ^{13}C NMR spectrum were observed, corresponding to ^{13}C-formate (Supplementary Fig. 1). Additionally, HMP formed with 1-^{13}C-HEP and 2-^{13}C-HEP was analysed by ^{31}P NMR spectroscopy, resulting in a doublet (from ^{13}C-HMP, Fig. 2a) and a singlet signal (from ^{12}C-HMP), respectively. The hydrogens at C1 are not removed in this process as the HEPD-catalysed oxidation of 1-$^{2}H_2$-HEP produced 1-$^{2}H_2$-HMP (Fig. 2a, inset).

The enzyme reaction was also performed in the presence of $^{18}O_2$ (99 atom %) with 2-^{13}C-HEP as substrate to circumvent complications from spurious formate5. After derivatization of formate to its *tert*-butyldimethylsilyl ester, the products were monitored by gas chromatography-mass spectrometry (GC-MS), displaying ions at *m/z* 106 and 104 corresponding to loss of the *tert*-butyl group (M-57) from derivatized ^{18}O,^{13}C-formate and ^{16}O,^{13}C-formate, respectively. The ^{18}O in formate exchanges with solvent in a time-dependent fashion in the protocol used (Supplementary Fig. 2), explaining the presence of the two products. The shortest exposure to the work-up and derivatization conditions resulted in >85% ^{18}O-formate (Fig. 2b). Incorporation of ^{18}O into HMP was assessed using LC-MS. Approximately 60% of HMP contained ^{18}O (*m/z* 115) with 40% containing ^{16}O (*m/z* 113) (Fig. 2c). This result was unexpected because the primary alcohol of HMP did not exchange under the reaction conditions. In an effort to understand the lower than expected ^{18}O content in HMP, the reaction was also performed in the presence of 80% (v/v) $H_2{}^{18}O$ (95 atom %)/$H_2{}^{16}O$. LC-MS analysis revealed 69% 2-^{16}O-HMP and 31% 2-^{18}O-HMP (Supplementary Fig. 3). When corrected for the ^{18}O content of the labeled water, the two complementary experiments ($^{18}O_2$ and $H_2{}^{18}O$) are in good agreement and suggest the intermediacy of a species in which oxygen derived from O_2 exchanges with water. These results also demonstrate that HEPD is a dioxygenase. The results of all labelling studies are summarized in Fig. 2d.

HEPD does not have sequence homology with other proteins in the databases except for enzymes that likely catalyze the same transformation judging from their operon context. To gain three-dimensional information, the structure of HEPD was determined by single wavelength anomalous diffraction data collected from crystals of selenomethionine incorporated protein, and refined to a Bragg limit of 1.8 Å. Crystallization was contingent on the presence of 50 mM $CdCl_2$ in the precipitant. The overall structure consists of imperfect tandem repeats of a bi-domain architecture (Fig. 3a). Each of the repeats is composed of an all ⟨-helical domain linked to a ®-barrel fold characteristic of the cupin superfamily6. Despite the lack of appreciable sequence similarity, each of the two repeats is structurally

homologous to the monomer of HppE[7], a non-heme iron-dependent enzyme that converts (*S*)-2-hydroxypropylphosphonic acid (2-HPP) to fosfomycin (Fig. 1). However, the repeats of HEPD are not entirely discretely folded domains as the ®-barrel domain of the first repeat is composed of interlacing ® strands from different parts of the molecule.

The disposition of the tandem domains of HEPD recapitulates many of the elements of the quarternary structure of HppE[7] with the tandem arrangement found in HEPD structurally analogous to one-half of the HppE tetramer. This tetramer is stabilised through crossover interactions between the ⟨-helical domains of the individual monomers. In contrast, the tandem arrangement in HEPD is held in place by two short orthogonal ⟨-helices located at the junction between each helical and ®-barrel domain (Fig. 3b). The ®-barrel fold of the first repeat contains all of the canonical active site elements of non-heme iron enzymes, including a 2 His-1 Glu facial triad3. A Cd(II) ion is situated at the base of the active site coordinated by His129, Glu176, and His182 (Fig. 3c). Well-defined spherical electron densities have been modeled as three water ligands resulting in a six-coordinate metal center. The constellation of metal ligands is similar to that of HppE, but the disposition of these ligands within the ®-barrel is not conserved as Glu176 of HEPD is situated on a different ®-strand than the equivalent Glu142 of HppE[7]. Furthermore, the spacing between the first two metal ligands in HEPD ($HX_{46}E$) is unique as these residues are closely spaced ($HX_{1\text{-}4}E/D$) in other facial triad enzymes7. In the second repeat in HEPD, the canonical 2 His-1 Asp/Glu is replaced by an arrangement of 2 His-1 Asn, and steric occlusion by residues Tyr358 and Lys404 precludes formation of a competent metal binding pocket. Combined with the observed requirement for one equivalent of iron for full enzyme activity, the second repeat is likely vestigial and does not participate in catalysis. Given the structural similarity to the epoxidase HppE, HEPD was incubated with 2-HPP, the substrate for HppE. 2-HPP was converted to 2-oxopropylphosphonate (2-OPP), rendering the enzyme inactive in the process (Supplementary Fig. 5). No evidence was found for hydrogen peroxide formation in this transformation.

Attempts to produce crystals of Fe(II)-HEPD have failed due to the high concentrations of Cd(II) required for crystallization. Crystals of SeMet labeled Cd(II)-HEPD were grown in the presence of HEP and solved to a resolution of 1.92 Å revealing electron density consistent with bidentate coordination of substrate to Cd^{2+} (Fig. 3d), which is similar to that observed for binding of 2-HPP to Co(II)-HppE[7]. In the HppE co-crystal structures, substrate binding induces substantial reorganization of the active site. In contrast, binding of HEP to Cd(II)-HEPD results only in the torsional movement of Tyr98 about χ1 resulting in a hydrogen bond interaction (2.3 Å) with one of the phosphonate oxygen atoms of the substrate. An additional hydrogen bond interaction occurs between N™2 of Asn126 (2.8 Å) and a different phosphonate oxygen.

While oxidative scission of carbon-carbon bonds is well documented, previously characterized proteins typically act on substrates that contain aromatic3, alkene8, or 1,2-dihydroxy functionalities9. No such activating groups are present in HEP, nor does HEPD need multiple successive oxidations such as in P450-mediated cleavage of the C20-C22 side chain of sterols10. Fig. 4 presents a working model for the HEPD reaction. The substrate is proposed to bind to Fe(II) in a bidentate fashion followed by reaction with O_2 resulting in a

Fe(III)-[O_2^-] intermediate. This species is proposed to abstract a hydrogen atom from C2 of HEP to generate intermediate II, akin to similar steps proposed for isopenicillin N synthase (IPNS) and *myo*-inositol oxygenase9,11. One important difference between IPNS and HEPD is that the former contains a sulfur ligand from the substrate that has been suggested based on computational studies to stabilize the Fe(III)-[O_2^-] intermediate and overcome the unfavorable energetics of O_2 binding and activation12. Although a thiolate ligand is lacking in HEPD, the observation that external electrons are not required leaves no alternate pathways to convert intermediate I into a more reactive species found in other non-heme iron oxygenases4. Furthermore, HEP does not have low energy electrons that can be provided by the substrate, as in the extradiol dioxygenases that utilize highly electron rich catechol substrates. HEPD also does not contain other nearby metals that are important for activity, in contrast to the binuclear iron enzyme *myo*-inositol oxygenase13. Hence, the only option for HEPD appears to be hydrogen atom abstraction from C2 by intermediate I to produce the hydroperoxo complex II and a substrate radical. Two different pathways can be envisioned to account for the labelling studies. The substrate radical could attack the hydroperoxide generating a ferryl species (Fe^{IV}=O) and a hemiacetal (Fig. 4). The latter can undergo a retro-Claisen type C-C bond scission with the incipient negative charge on C1 attacking the electrophilic ferryl, potentially via a Horner-Wadsworth-Emmons-like intermediate stabilized by metal coordination. A ferryl would account for the required intermediacy of a species in which oxygen derived from O_2 can exchange with solvent14-19 (Supplementary Fig. 6). A second mechanism that can account for the observed data involves conversion of intermediate II to the hydroperoxide III, which can undergo a Criegee-type rearrangement to provide the formate ester of HMP (Fig. 4). Hydrolysis of this ester is expected to occur at the carbonyl carbon, but such a mechanism would not account for the incorporation of oxygen derived from solvent into HMP. This observation can be explained if hydrolysis took place via attack at C1 by solvent exchangeable hydroxide released in the Criegee rearrangement. Both models can also explain the observed conversion of 2-HPP into 2-OPP, with the additional methyl group in the substrate inducing the cleavage of a C-O bond instead of C-C bond to form a ketone (Supplementary Fig. 7). However, the lack of hydrogen peroxide production in this latter transformation favors the hydroxylation mechanism over the hydroperoxylation model. Further studies will be required to provide insights into the factors that result in epoxide formation by HppE and C-C bond cleavage by HEPD.

Methods Summary

HEPD was purified by immobilized metal affinity chromatography (IMAC). Iron analysis22 on the as-isolated protein revealed iron content below the detection limits (0.05 equiv.) whereas fully active, Fe(II)-reconstituted protein contained 0.99 ± 0.05 equivalent of Fe per polypeptide. Typical aerobic assays contained, in a final volume of 1000 μL: 50 mM K+-HEPES, pH 7.5, 2-10 μM HEPD, 5-10 mM HEP or isotopically labeled HEP. Formate produced was derivatized at 20 °C using 0.5 mL N-methyl-N-[*tert*-butyldimethylsilyl]trifluoroacetamide (MTBSTFA) + 0.1% tert-butyldimethylsilyl chloride (TBDMSCl) for 20 min and monitored by GC-MS. HMP produced was analyzed by LC-MS using atmospheric pressure chemical ionization (APCI). The stoichiometry of formate to

HMP produced during the HEPD reaction was determined by ^{13}C NMR spectroscopy. The potential for ^{18}O incorporation from H_2O into HMP was evaluated by running the reaction in $H_2{}^{18}O$. HEPD was anaerobically activated as described in the Methods section. The mixture (150 μL) was removed from the glove box and added to an aerobic mixture of $H_2{}^{18}O$ (832.6 μL, 95 atom %), and HEP (17.4 μL). The final concentrations of HEPD and HEP were 10.5 μM and 3 mM, respectively. $H_2{}^{18}O$ was diluted to 79% in the 1 mL reaction. Intermittent bubbling of O_2 enabled the complete consumption of HEP over 1 h. HMP produced was analyzed and a representative isotopic distribution of $^{18}O/^{16}O$ is shown in Supplementary Figure 3. The reported percentage of ^{18}O-HMP is corrected based on the amount of $H_2{}^{18}O$ in the assay.

Methods

Purification of Recombinant HEPD

Recombinant HEPD was overexpressed as previously described2. HEPD was purified by IMAC using a Ni-NTA matrix (Qiagen; Valencia, CA). In a typical purification, 10 g of cells were thawed in 30 mL of Buffer A (50 mM HEPES, pH 7.5, 300 mM NaCl, 20 mM imidazole, 10% glycerol), and allowed to incubate with lysozyme (1 mg mL^{-1}) for 30 min at 4 °C. Cells were lysed by two passages through a French press at a setting of 20,000 psi, and the lysate was centrifuged at 35,000×g for 1 h at 4 °C. The supernatant was loaded onto a Ni-NTA column (1.5 × 3 cm) equilibrated in Buffer A, and the column was washed with 10 column volumes of Buffer A. The column was subsequently washed with Buffer A containing 50 mM and 100 mM imidazole. The remaining bound protein was eluted with Buffer A containing 250 mM imidazole. HEPD typically elutes between 100-250 mM imidazole and was pooled based on SDS-PAGE analysis. The protein was concentrated using an Amicon ultracentrifugation device with a 10 kDa membrane cutoff, and the buffer was exchanged to 50 mM HEPES, pH 7.5, 300 mM NaCl, 10% glycerol by gel filtration. Protein concentrations were determined by Bradford analysis using bovine serum albumin as a standard. The protein was frozen in 100 μL aliquots and stored at -80 °C until ready for use.

HEPD Activity Assay

Anaerobic activation of HEPD was achieved in an anaerobic chamber obtained from Coy Laboratory Products, Inc. (Grass Lake, MI) under an atmosphere of N_2 and H_2 (95% /5%). HEPD (30-70 μM) was treated with one molar equivalent of $Fe(II)(NH_4)_2(SO_4)_2$ for 20 min in a final volume of 200 μL. The solution was subsequently brought outside the glove box and combined with the remaining assay components. The reaction was initiated by addition of HEP (see Methods Summary above for assay ingredients). For the quantification of formate, 150 μL aliquots of the assay mixture were removed at designated times and added to 2 μL of 9.2 M H_2SO_4 to quench the reaction. Precipitated protein was pelleted by centrifugation, and 50 μL of the supernatant was analyzed by HPLC (Agilent Technologies 1200 series HPLC). Formate was chromatographed using an AMINEX HPX-87H (BioRad) column (300 × 7.8 mm) in an isocratic mobile phase (25 mN H_2SO_4). The flow rate and temperature were 0.6 mL min^{-1} and 60 °C, respectively. Formate eluted at 14.1 min.

Formate Analysis by GC-MS

Formate production was monitored on an Agilent 6890N (Agilent Technologies, Palo Alto, CA, USA) gas chromatograph with helium carrier gas. Sample introduction was via split injection onto a HP-5 (5%-phenyl-methyl-polylsiloxane) column (30 m, 0.32 mm i.d., 0.25 μm film thickness). The injection temperature was 250 °C. The initial column temperature was 40 °C, and was held for 5 min after injection before increasing to 230 °C at 15 °C min^{-1}. The temperature was held at 230 °C for the remainder of the 27 min program. The HEPD reaction was performed as described above. Sulfuric acid was added to a final concentration of 0.12 M to quench the reaction. The acidified solutions were subjected to three separate 0.5 mL diethyl ether extractions. The extracts were combined and formate was derivatized using 0.5 mL MTBSTFA + 0.1% TBDMSCl (Pierce). Typical derivatizations were performed for 20 min at 25 °C. The solution (1-2 μL) was then directly injected into the GC-MS. Under the given GC conditions derivatized formate had a retention time of 7.4 min.

HMP Analysis by LC-MS

Analysis and quantitation of HMP was carried out by LC-MS using an Agilent 1200 series LC-MS equipped with a multimode electrospray ionization/APCI spray chamber. For HMP, APCI ionization was performed using positive ionization and chromatographic separations were achieved using a 150 × 4.6 mm Synergi C18 Fusion-RP column with a 4 μm particle size (Phenomenex®, Torrance, California, USA). HMP has a retention time of approximately 6 min at a flow rate of 0.5 mL/min using a 0.1 % formic acid isocratic mobile phase. Injection volumes ranged from 5-15 μL. The nebulizer gas was N_2 at 8 L/min with a nebulizer pressure of 40 psi. The drying gas temperature was 300 °C and the vaporization temperature was 250 °C. The capillary and charging voltages were both set to 2000 V and the corona discharge current was 4 μA. The gain was set to 1.0 and the fragmentor voltage was 70 V.

Analysis of HEPD Products by NMR Spectroscopy

^{1}H-coupled ^{31}P-NMR, and ^{1}H-decoupled ^{31}P-NMR analyses were performed on a Varian Inova 600 spectrometer equipped with a 5-mm Varian 600DB AutoX probe with ProTune accessory tuned for phosphorus at 242.79 MHz. ^{13}C spectra were recorded on a Varian Unity 500 spectrometer. Carbon chemical shifts were referenced to an external standard of 0.1% tetramethylsilane in $CDCl_3$. Phosphorus chemical shifts are reported relative to an external standard of 85% phosphoric acid ($\delta = 0$). HEPD assays were performed as described above except that the reaction was terminated by removal of the protein by an ultrafiltration device (Millipore Amicon) equipped with a 10 kDa molecular weight cutoff membrane. D_2O was then added to the sample to a final concentration of 20% prior to data acquisition. The identification of the second product as formate was established by ^{13}C NMR and GC-MS as seen in Supplementary Figure 1A and B.

$^{18}O_2$ Incorporation Assay

Assays utilizing $^{18}O_2$ were carried out as described. All assay components were prepared and mixed anaerobically. 2-^{13}C-HEP was substituted for HEP so that formate derived from substrate could be differentiated from spurious formate during GC-MS analysis. The glass

vial was fitted with a tight rubber septum and brought outside of the glove box. The reaction was initiated by the introduction of 1 mL of $^{18}O_2$ (99 atom %, Isotec) via gas-tight syringe. The solution was allowed to slowly stir at room temperature for 90 min at which time sulfuric acid was added to a final concentration of 92 mM to quench the reaction. After centrifugation to remove precipitated protein, HMP was directly analyzed by LC-MS. Formate was extracted and derivatized as described above prior to GC-MS analysis. Time-dependent washout of the ^{18}O-label in formate, under acidic conditions, was observed by GC-MS (Supplementary Figure 2) and has been noted elsewhere23.

Supplementary Material

Refer to Web version on PubMed Central for supplementary material.

Acknowledgments

We thank Benjamin Griffin (UIUC), J. Martin Bollinger (Penn State), Scott E. Denmark (UIUC), and Tadgh Begley (Cornell) for helpful discussions. This work was supported by grants from the National Institutes of Health (PO1 GM077596 to W.W.M., W.A.V., and S.K.N. and NIH RO1 GM59334 to W.W.M.) and by the University of Illinois. The PDB accession codes for the structures reported here are 3G7D for the apo structure and 3GBF for the liganded structure.

References Cited in Methods

1. Seto H, Kuzuyama T. Bioactive Natural Products with Carbon-Phosphorus Bonds and Their Biosynthesis. Nat Prod Rep. 1999; 16:589–596. [PubMed: 10584333]
2. Blodgett JA, et al. Unusual transformations in the biosynthesis of the antibiotic phosphinothricin tripeptide. Nat Chem Biol. 2007; 3:480–5. [PubMed: 17632514]
3. Costas M, Mehn MP, Jensen MP, Que L Jr. Dioxygen activation at mononuclear nonheme iron active sites: enzymes, models, and intermediates. Chem Rev. 2004; 104:939–86. [PubMed: 14871146]
4. Kovaleva EG, Lipscomb JD. Versatility of biological non-heme Fe(II) centers in oxygen activation reactions. Nat Chem Biol. 2008; 4:186–93. [PubMed: 18277980]
5. Shyadehi AZ, et al. The mechanism of the acyl-carbon bond cleavage reaction catalyzed by recombinant sterol 14 alpha-demethylase of Candida albicans. J Biol Chem. 1996; 271:12445–50. [PubMed: 8647850]
6. Dunwell JM, Purvis A, Khuri S. Cupins: the most functionally diverse protein superfamily? Phytochemistry. 2004; 65:7–17. [PubMed: 14697267]
7. Higgins LJ, Yan F, Liu P, Liu HW, Drennan CL. Structural insight into antibiotic fosfomycin biosynthesis by a mononuclear iron enzyme. Nature. 2005; 437:838–44. [PubMed: 16015285]
8. Grogan G. Emergent mechanistic diversity of enzyme-catalysed beta-diketone cleavage. Biochem J. 2005; 388:721–30. [PubMed: 15934927]
9. Xing G, et al. Evidence for C-H cleavage by an iron-superoxide complex in the glycol cleavage reaction catalyzed by myo-inositol oxygenase. Proc Natl Acad Sci USA. 2006; 103:6130–5. [PubMed: 16606846]
10. Lieberman S, Lin YY. Reflections on sterol sidechain cleavage process catalyzed by cytochrome P450(scc). J Steroid Biochem Mol Biol. 2001; 78:1–14. [PubMed: 11530278]
11. Burzlaff NI, et al. The reaction cycle of isopenicillin N synthase observed by X-ray diffraction. Nature. 1999; 401:721–4. [PubMed: 10537113]
12. Brown CD, Neidig ML, Neibergall MB, Lipscomb JD, Solomon EI. VTVH-MCD and DFT studies of thiolate bonding to $[FeNO]^7$/$[FeO_2]^8$ complexes of isopenicillin N synthase: substrate determination of oxidase versus oxygenase activity in nonheme Fe enzymes. J Am Chem Soc. 2007; 129:7427–38. [PubMed: 17506560]

13. Xing G, et al. Oxygen activation by a mixed-valent, diiron(II/III) cluster in the glycol cleavage reaction catalyzed by myo-inositol oxygenase. Biochemistry. 2006; 45:5402–12. [PubMed: 16634621]
14. Kikuchi Y, Suzuki Y, Tamiya N. The source of oxygen in the reaction catalysed by collagen lysyl hydroxylase. Biochem J. 1983; 213:507–12. [PubMed: 6412686]
15. Baldwin JE, Adlington RM, Crouch NP, Pereira IAC. Incorporation of ^{18}O-Labelled Water into Oxygenated Products Produced by the Enzyme Deacteoxy/deacetylcephalosporin C Synthase. Tetrahedron. 1993; 49:7499–7518.
16. Sabourin PJ, Bieber LL. The mechanism of alpha-ketoisocaproate oxygenase. Formation of beta-hydroxyisovalerate from alpha-ketoisocaproate. J Biol Chem. 1982; 257:7468–71. [PubMed: 7085633]
17. Lindblad B, Lindstedt G, Lindstedt S. The mechanism of enzymic formation of homogentisate from p-hydroxyphenylpyruvate. J Am Chem Soc. 1970; 92:7446–9. [PubMed: 5487549]
18. Wackett LP, Kwart LD, Gibson DT. Benzylic monooxygenation catalyzed by toluene dioxygenase from Pseudomonas putida. Biochemistry. 1988; 27:1360–7. [PubMed: 3365392]
19. Pestovsky O, Bakac A. Aqueous ferryl(IV) ion: kinetics of oxygen atom transfer to substrates and oxo exchange with solvent water. Inorg Chem. 2006; 45:814–20. [PubMed: 16411719]
20. Woodyer RD, Li G, Zhao H, van der Donk WA. New Insight into the Biosynthesis of Fosfomycin: Discovery of the Missing Link Illuminates the Mechanism of Methyl Transfer. Chem Commun. 2007:359–361.
21. Liu P, et al. Protein purification and function assignment of the epoxidase catalyzing the formation of fosfomycin. J Am Chem Soc. 2001; 123:4619–20. [PubMed: 11457256]
22. Beinert H. Micro methods for the quantitative determination of iron and copper in biological material. Methods Enzymol. 1978; 54:435–45. [PubMed: 732579]
23. Shyadehi AZ, et al. The mechanism of the acyl-carbon bond cleavage reaction catalyzed by recombinant sterol 14 alpha-demethylase of Candida albicans. J Biol Chem. 1996; 271:12445–50. [PubMed: 8647850]

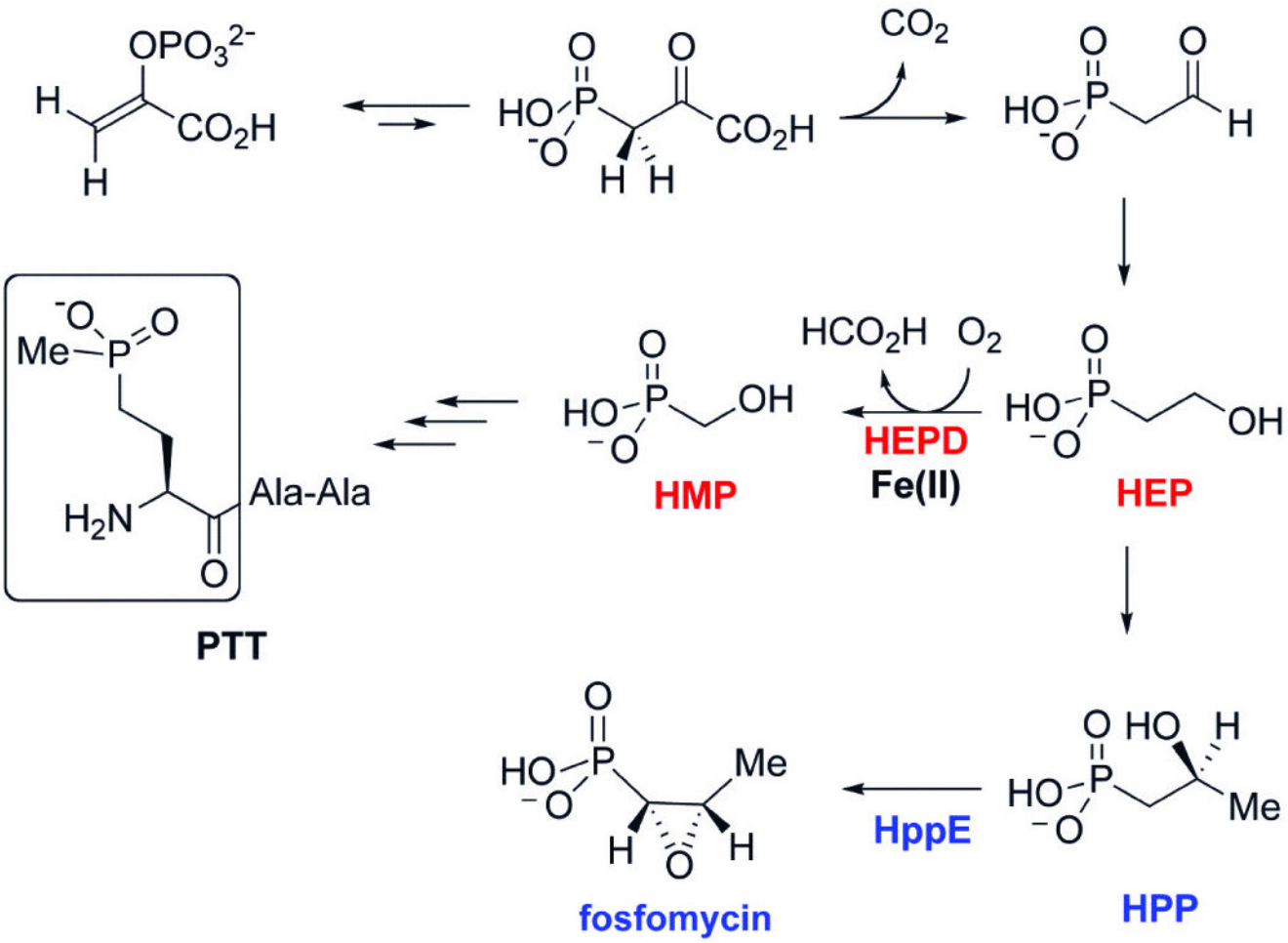

Figure 1. Structure of PTT and the reaction catalyzed by HEPD

The biosyntheses of the commercial herbicide phosphinothricin (boxed in the PTT structure) and the clinically used antibiotic fosfomycin share several early steps starting with phosphoenolpyruvate before the pathways diverge after formation of HEP.2,20 HEPD catalyzes the unprecedented conversion of HEP to HMP (for the steps from HMP to PTT, see Supplementary Fig. 8). The structurally related enzyme HppE converts HPP to fosfomycin21.

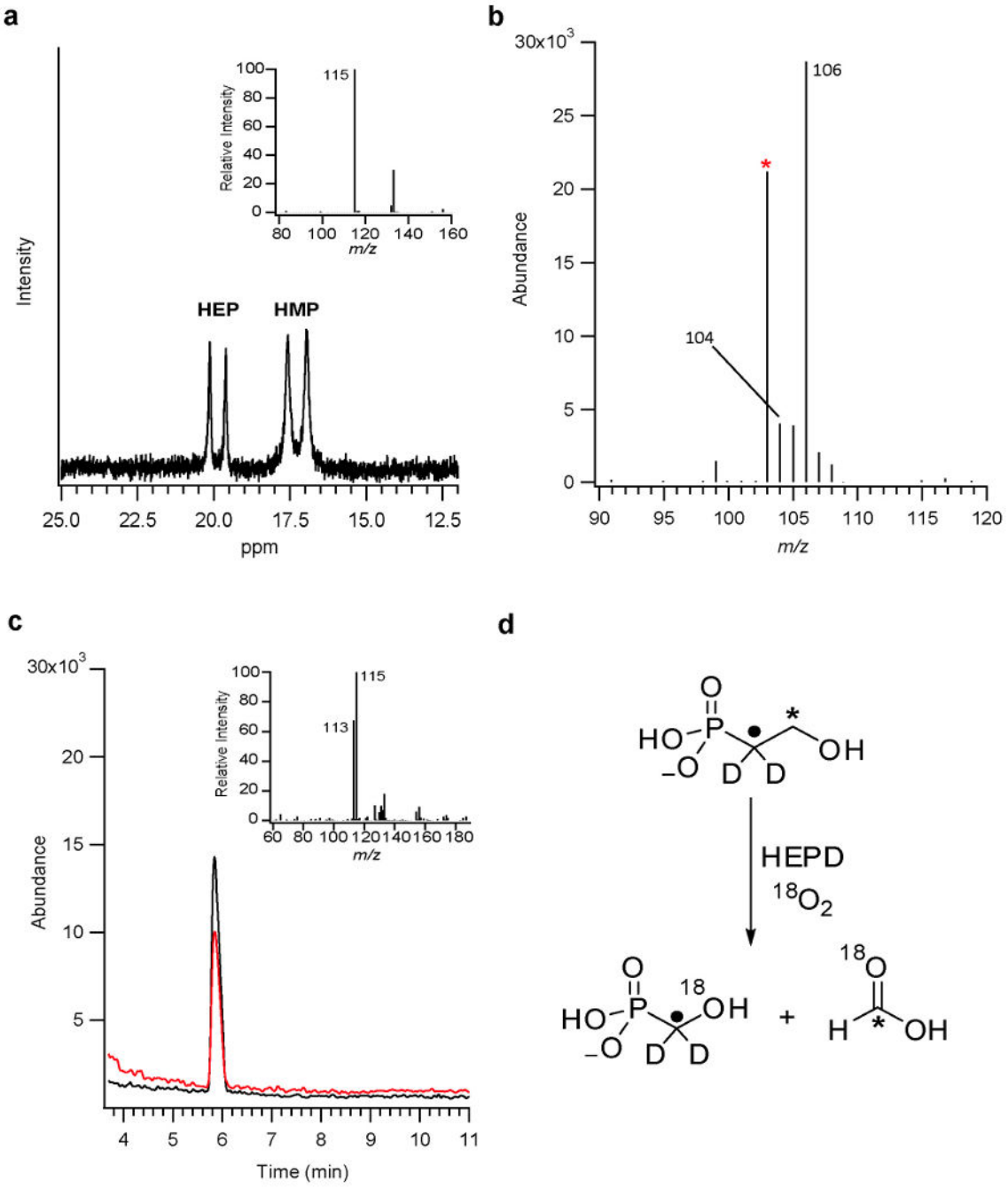

Figure 2. NMR and mass spectral data from *in vitro* labelling studies

a, ^{31}P NMR spectrum showing production of ^{13}C-HMP (δ 17.2 ppm) from 1-^{13}C-HEP (δ 19.9 ppm) after 50% conversion. Inset: mass spectrum of HMP derived from a reaction utilizing 1,1-$^{2}H_2$-HEP. **b,** Mass spectrum of ^{18}O,^{13}C-formate (*m/z* 106) produced by HEPD from a reaction utilizing $^{18}O_2$ and 2-^{13}C-HEP. Spurious formate is denoted by an asterisk (*m/z* 103). **c,** Analysis of HMP produced from the HEPD reaction performed with $^{18}O_2$. Extracted ion chromatograms demonstrate ~60 % of the HMP contains ^{18}O (black line)

while 40 % contains ^{16}O (red line). Inset: summed mass spectrum from the total ion chromatographic peak. **d,** Summary of labelling studies from the HEPD reaction.

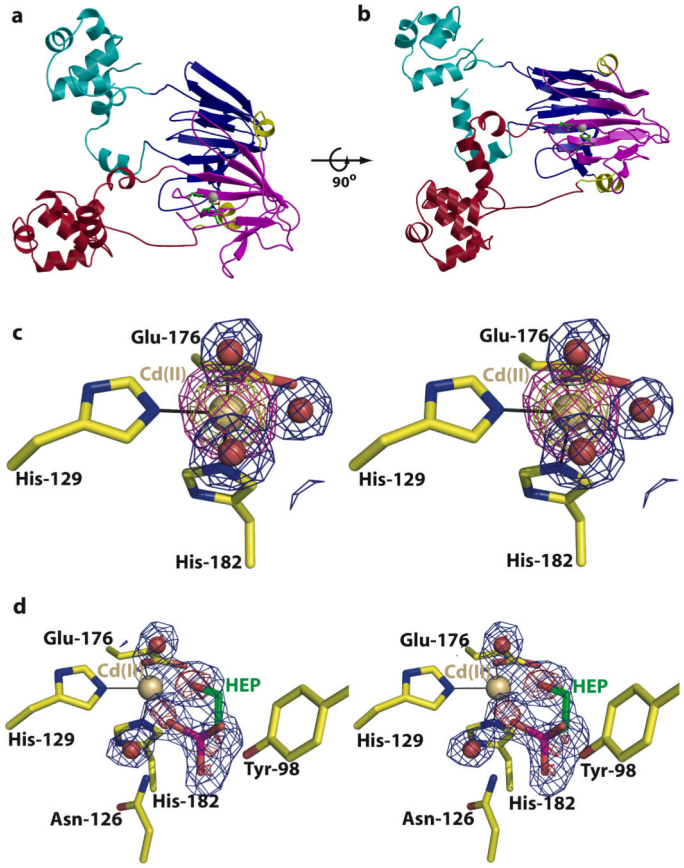

Figure 3. Structures of Cd(II)-HEPD and Cd(II)-HEPD/HEP

a and b, Orthogonal views of Cd(II)-HEPD showing the tandem arrangement of the HppE fold including cupin domains (blue and purple), α-helical domains (red and cyan), cadmium (white sphere), and metal ligands (green). **c,** Stereoview of electron density maps using model phases ($F_o - F_c$). The first map (contoured at 3σ in blue) was calculated by omitting metal-bound solvents (red sphere) prior to one round of refinement. The second map, contoured at 5σ (purple mesh) and 14σ (yellow mesh), was calculated by omitting the cadmium (gold sphere) prior to one round of refinement. **d,** Stereoview electron density maps ($F_o - F_c$) calculated using HEPD-HEP model phases. The map is calculated by omitting metal-bound ligands prior to one round of refinement (contoured at 3σ in blue mesh and 6σ in red). HEP carbons shown in green.

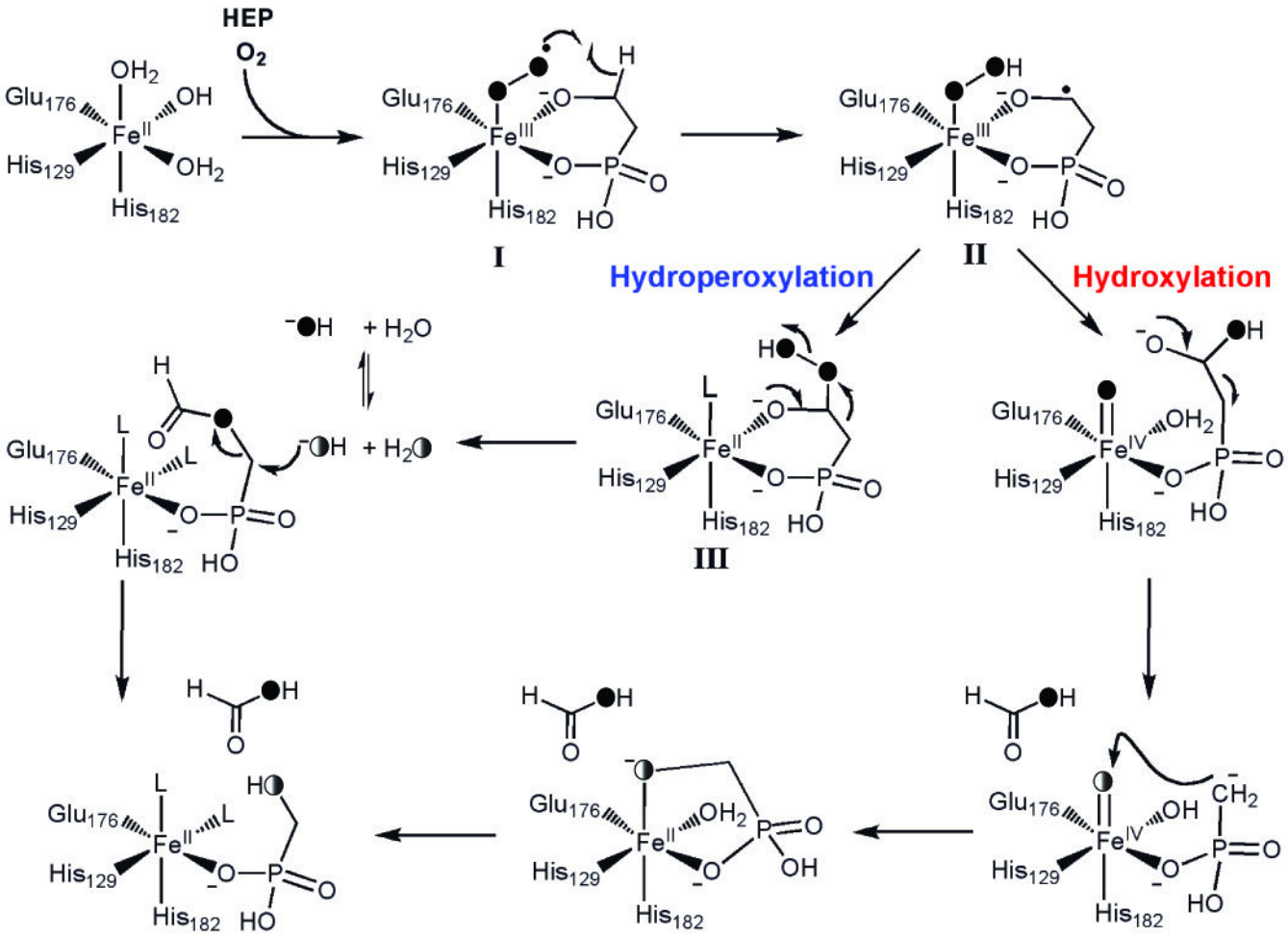

Figure 4. Working models for the mechanism of catalysis by HEPD

The ferrous ion reacts with O_2 to generate the formal ferric-superoxide complex I. Hydrogen atom abstraction from C2 of HEP generates a substrate radical and ferric-hydroperoxide (II). From intermediate II two possible pathways can be envisaged. Radical attack on the ferric-hydroperoxide may cleave the O-O bond and produce a ferryl species and a hemiacetal (hydroxylation). C-C bond cleavage and attack of the resulting resonance stabilized anion at the ferryl generates formate and HMP. The weak hemiacetal ligand is posited to first dissociate from the iron to account for solvent exchange (Supplementary Fig. 6). Alternatively, intermediate II could be converted to the alkyl hydroperoxide III (hydroperoxylation), which can undergo a Criegee-type rearrangement to generate formyl-HMP. Hydrolysis must then occur at the methylene carbon to account for the oxygen labelling studies.